Fabrication and Assembly Performance of the First 4.2 m MQXFA Magnet and Mechanical Model for the Hi-Lumi LHC Upgrade

D. W. Cheng, G. Ambrosio, E.C. Anderssen, N. Bourcey, H. Felice, P. Ferracin, P. Grosclaude, M. Guinchard, J.C. Perez, H. Pan, S.O. Prestemon, G. Vallone

Abstract—The LHC Accelerator Research Program (LARP), in collaboration with CERN and under the scope of the high luminosity upgrade of the Large Hadron Collider, is in the prototyping stage in the development of a 150 mm aperture high-field Nb_3Sn quadrupole magnet called MQXF. This magnet is mechanically supported using a shell-based support structure, which has been extensively demonstrated on several R&D models within LARP, as well as in the more recent short (1.2 m magnetic length) MQXF model program. The MQXFA magnets are each 4.2 m magnetic length, and the first mechanical long model, MQXFA1M (using aluminum surrogate coils), and MQXFA1 prototype magnet (the first prototype with Nb_3Sn coils) have been assembled at LBNL. In this paper, we summarize the tooling and the assembly processes, and discuss the mechanical performance of these first two assemblies, comparing strain gauge data with finite element model analysis, as well as the near-term plans for the long MQXF magnet program.

Index Terms— Superconducting magnet, superconducting coils, High Luminosity LHC, MQXF, quadrupole

I. INTRODUCTION

THE development of the MQXF inner triplet quadrupoles for the High Luminosity LHC upgrade has been a major effort of the LHC Accelerator Research Program (LARP) collaboration in partnership with CERN [1], [2]. Based on a series of technology development models [3]-[6] and most recently the MQXFS structures, 1.2 m magnetic length models of the same cross section [7] [8], the MQXFA structure is a 4.2 m magnetic length quadrupole with a 150 mm bore. The actual yoke length from end to end is 4.56 m long, not includ-
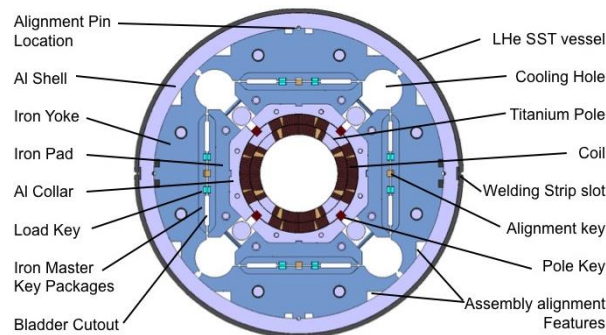

Fig. 1. Cross section of the MQXFA Magnet (the LHe SST vessel will be added during cold mass assembly).

ing the splice connections and axial loading hardware. The magnet is designed with the bladder-and-key technology [9] which uses an aluminum shell to provide the coil preload through the use of interference keys and different CTE of the structural materials to provide the rest of the preload force during the cooldown of magnet to 1.9 K. See Fig. 1 for the cross sectional layout. The magnet design and parameters are discussed in [2].

Although long mirror magnet structures have qualified individual long coils fabrication [10], [11], the MQXFA is the first long Nb_3Sn quadrupole magnet built since the 3.7 m long LQ [5] model magnet was successfully tested, and whose development experience was fundamental to the length scale-up of Nb_3Sn magnets. As such, the first assembly of this structure was a mechanical model, MQXFA1M, which used aluminum "surrogate" coils instead of real Nb_3Sn coils in the assembly processes. These instrumented surrogate coils were used to verify the preload operations and also to qualify the new scaled-up assembly tooling, which was based on the MQXFS assemblies experience [12], without risking damage to real coils. The real magnet, MQXFA1, was assembled once these assembly processes were qualified.

In this paper we present the mechanical performance of these two structures, MQXFA1M and MQXFA1, describe the experiences gained from the use of scaled-up tooling and processes to assemble them, and present the status and plans to move forward with these magnets in the context of the High Luminosity LHC Accelerator Upgrade Project (HL-LHC AUP).
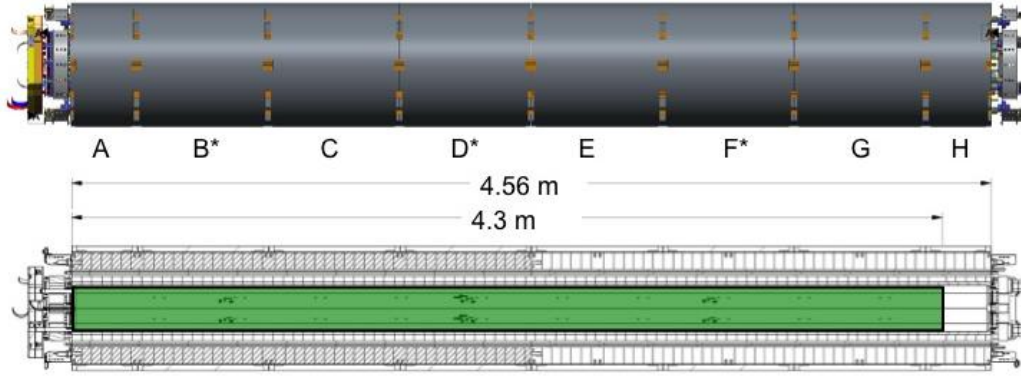
Fig. 2. (Top) The MQXFA1 magnet shell arrangement. * Indicates shells that were instrumented. (Bot) The length of the MQXFA1 real coils dimensioned in the structure.

II. MQXFA1M MECHANICAL ASSEMBLY

While the MQXFA1M mechanical model is only a test assembly, all the components are part of the final assembly with the exception of the aluminum surrogate coils, which are swapped for the real coils. This structure will only be assembled and preloaded at RT; it will not be cooled down. One important difference between the real and surrogate coils for this assembly, however, is that the real coils were initially designed with a 4.0 m magnetic length and were in production when a design review recommended increasing the operating margin of the inner triplet quadrupoles by increasing the magnetic length to 4.2 m. Therefore, while these first coils are ~4.3 m long the surrogate and all subsequent coils will be ~4.5 m long coils to accommodate the longer magnetic length. See Fig. 2.

A. Shell-Yoke Subassembly

1) Shell Segments

The shells are made of heat-treated 7075 aluminum alloy. To help with the stability of the shells during machining, it was recommended that the 7075 alloy be heat treated to a T652 condition which essentially adds a mechanical stress relieve step to a normal T6 condition. However, capacity issues limited this heat treatment to the two short (325 mm) shell segments; the six long (651 mm) shells were treated to the T6 condition only. All the shells were machined without issue, nonetheless.

Upon receipt each individual shell had its roundness and average inner diameter measured in the free state at 5 axial locations along the length of each shell. Table I lists the arrangement order, based on minimizing the variance between adjacent shells. The resulting arrangement approximates an hourglass shape along the length, with the largest diameters on each end. The maximum variance of all shells was 61 μm on the ID, which represents a ~5% variation in coil preload stress based on the tolerance analyses described in [13].

Additionally, based on this arrangement, three of the shells were instrumented with strain gauges. Two types of strain gauges are used to measure both axial and azimuthal strains:

TABLE I
SHELL DIAMETERS AND THEIR ORDERING ARRANGEMENT

Shell	Shell ID	Avg. Dia., mm	Instrumented	Gauge vendor
A	Short 1	556.001		
B	Long 6	555.986	Yes	Vishay
C	Long 4	555.973		
D	Long 2	555.971	Yes	Vishay/HBM
E	Long 5	555.951		
F	Long 1	555.978	Yes	Vishay
G	Long 3	556.000		
H	Short 2	556.018		

DC-powered full-bridge circuits ("Vishay") were mounted on each shell, while AC-powered half-bridge circuits ("HBM") were also mounted only on the second, central shell. Fig. 2 also shows the locations of these strain gauges.

2) Shell-Yoke Halves

The full-length shell-yoke assembly is made up of two half-length subassemblies before being assembled into a full-length assembly. The process started in the vertical orientation, where three long shells and one short shell were stacked on the assembly stand. The yokes were procured as primarily 49 mm thick A36 steel laminations that were stacked into eight quadrant subassemblies, each one half the length (~2.3 m) of a full structure. These yoke quadrants were then inserted into the stacked shells, clamped into position, and then bladders and their supports were inserted into the cooling holes in preparation to insert the gap interference keys. See Fig 3.

Nominally, there is a 12 mm gap between each yoke quadrant but a small interference is required to complete these half-length subassemblies. 28 MPa (4100 psi) of bladder pressure was required to insert 100 μm of interference, or 12.1 mm total, in yoke gaps of both LE and RE halves. The shell strains reported were +158 με (average of "B" & "D" shells) and +260 με ("F" shell). This equates to ~210 +/-50 με over the assembly, and likely reflects the fabrication tolerances.

3) Assembling the Full-Length Shell-Yoke

The two half-length assemblies were rotated horizontally and placed on the magnet integration table. The tie rods of the half-length yoke stacks were then removed, the central bushings replaced, the halves pushed together, and finally full length tie rods were inserted through both halves. The final

Fig. 3. Shell and Yoke subassembly. (a) The shells are stacked onto the assembly stand. (b) The yoke stacks are inserted. (c) The yokes are clamped and aligned in place. (d) Bladders and their supports are inserted into the four cooling holes, pressurized, and gap keys installed. (e) The half-length subassembly is rotated horizontal prior to joining with the other half.

operation used a hydraulic tensioning rig attached to each rod, which stretches them to a minimum of 40 kN (9000 lbs.) each before tightening the lock nuts.

Unfortunately, during the tensioning operation the high pressure pump gauge was read incorrectly and the maximum tension applied actually reached 57 kN (12,900 lbs.). The pressure was released back to 40 kN per rod and the lock nuts tightened. After analyzing the conditions, we determined that no permanent damage occurred, as this was approximately 3% over the reported yield strength per the material certs, and therefore assembly processes continued.

B. Coil Pack Subassembly

1) Dressed Surrogate Coils

A "dressed" coil is one that has been instrumented with strain gauges in three axial locations and has ground plane insulation (GPI) applied to the O.D. and midplane surfaces. The GPI is a laminate of 75 μm polyimide + 38 μm B-stage epoxy adhesive applied to the coil with heat. As with the shells, DC-powered full-bridge circuits were mounted at all three locations, while AC-powered half-bridge circuits were also mounted in the center station only.

Each of the four aluminum surrogate coils was actually made in two half-length segments, approximately 2.3 m long each. Segments were paired to maintain as uniform a size as possible over the 4.5 m length, based on CMM profile data taken for all parts; thirteen profiles are measured along the length of a coil, three of which match with shell gauge locations: 740 mm, 1940 mm, and 3140 mm from the LE.
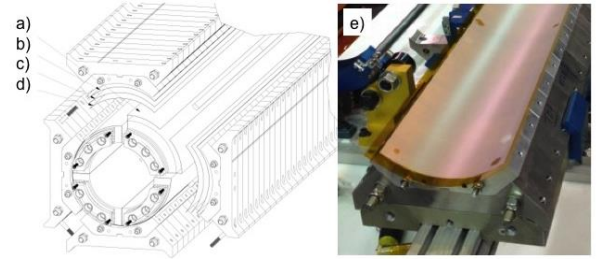

Fig 4. Radial buildup of coil pack. (a) Coil GPI. (b) Collar GPI. (c) G11 Radial shim. (d) Polyimide radial shim, and or pressure-sensitive film. (e) Pad-collar assembly with radial shims applied.

2) Pad-Collar Stacks

In a departure from the short model assembly processes described in [12], the aluminum collar laminations were preassembled onto the steel load pad lamination stacks to create a single full-length pad-collar structure. This simplifies the build process, because the bolted collar pack utilized in the short models is no longer needed as a separate assembly step. Radial shims of G11 and polyimide are applied to the collar surface, based on coil measurements. A further departure and simplification to the build process was to bolt every 7th pad lamination along the length rather than bolting every one.

3) Radial Shims and Assembly

The outer radius of a real impregnated coil is nominally 113.376 mm, which is the same as that of the surrogate coils. Variances of radius and midplane features of real components affect the amount of shims required to build up a coil pack. CMM profile measurements showed that these surrogate coils had an effective larger radius of 113.7 mm, and the coil pack radial shim packaging was developed from this value. As usual, pressure-sensitive film used in the first coil pack assemblies confirms whether the radial contact is adequate, and adjustments would be made if necessary. See Fig. 4.

The coil pack assembly was built up twice, both times using pressure sensitive film. One of the issues discovered was that by bolting every 7th lamination we were unable to obtain clear readings from the pressure sensitive film. This will be discussed further later in this paper.

The gaps between the collars were measured on the first build in order to properly shim the coil pole alignment keys on the second build. The pole keys were shimmed 0.4 mm per side, and measurements confirmed that the gap was closed between the keys and collars. See Table II for the final build parameters.

TABLE II
FINAL RADIAL BUILD UP FOR MQXFA1M COILS

Radial Element	Coils* L1+R3	Coils* L2+R4	Coils* L3+R2	Coils* L4+R1
GPI	115 μm (Polyimide + B-stage)			
Coil Specific shims	0	0	0	0
Pressure Sensitive film	175 μm			
Radial shim	125 μm G11 + 50 μm Polyimide			

*Coil pairs are made of a LE segment (L) and a RE segment (R).

C. MQXFA1M Integration and Preload

The MQXFA1M preload targets were based on FEA simulations at a magnet operating gradient of 130 T/m [14] where the following conditions must be met:

- The pole turns remain in contact with the pole with a pressure of 2 MPa at the mid-radius.
- Coil peak stress is limited to 150 MPa at 293 K and 200 MPa at 1.9 K.
- Maintain the stress in the support structure components within the material limits.

As a mechanical structure only, the corresponding shell azimuthal strain target for MQXFA1M at RT is 1300 µε in tension, and -1290 µε in the surrogate coils. This target corresponds to 525 µm of key interference w.r.t. nominal. See Fig. 5.

The actual amount of interference achieved was 450 µm when, due to a leaking bladder and extremely tight assembly schedule, we decided to take additional data points during the removal of load key shims during disassembly after replacing the bladder. As seen in the transfer function plots, the loading of the mechanical model matched the FEA results very closely; see Fig 6. Note that, unlike the results from the MQXFS models, the two different strain gauge systems did not seem to match as well. The HBM system was a new purchase prior to this assembly activity and we are examining whether incorrect system settings are contributing to the variance observed.

The axial preload operations were also removed due to this tight schedule. This was considered a low risk operation, even
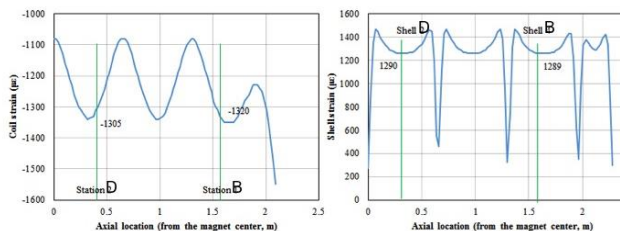

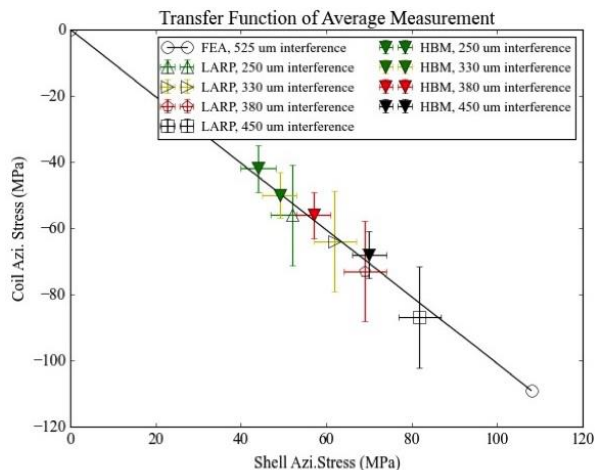Fig. 5. Strain targets for both shell and surrogate coils for MQXFA1M.

Fig 6. Transfer function of shell vs. coil for MQXFA1M. Measurements at 330 µm were taken during the disassembly process.

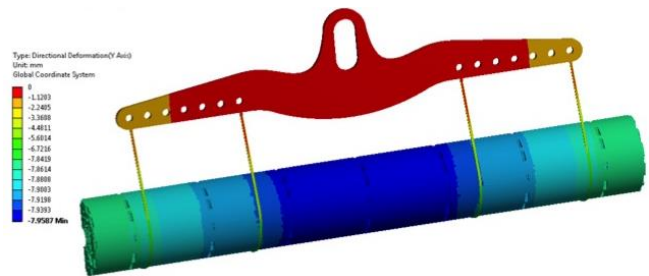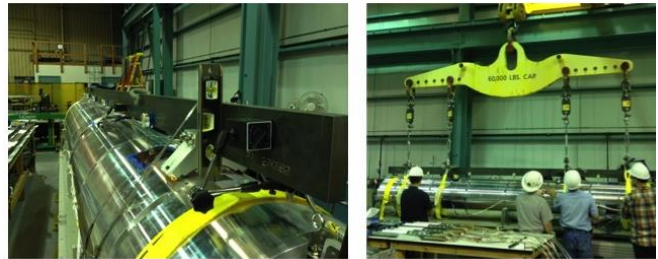Fig. 7. FEA result of the lifting system in 2g load case. Max deflection is 110 µm.

Fig. 8. (L) Simply supported beam with dial indicators measuring deflections. (R) Test lift operation.

though the rod material changed from 36 mm diameter 7075 Al in the MQXFS magnets to 32 mm diameter 316L stainless steel for MQXFA. This material also changed in the scale up from TQ to LQ [3], [5], and increases the annular clearance between the pads and rods for better cooling [15].

D. Magnet Lifting

One critical test employed after the magnet was assembled was the lifting operation of the 6800 kg (15000 lbs.) structure. Of concern was that the central shell segments were not spanned by a yoke lamination, as this was the interface between the two subassemblies. The governing criteria for lifting were limiting coil strain to a maximum of 500 µε and that there would be no separation between the central yoke segments. FEA of a conservative 2g case using a four-point pick showed that coil strain was ~20 µε, deflection of the structure was ~110 µm in the center, and there was no separation between the central yoke segments. See Fig. 7.

A matched set of lifting slings, turnbuckles and four load cells were purchased specifically for this lifting operation. To measure deflections a simply-supported beam was used to measure deflections with dial indicators. The test lift showed there was approximately 25 microns of deflection, and the strain gauges showed negligible changes during the operation. See Fig. 8.

At this point MQXFA1M was disassembled. All processes for the disassembly process were tested without issue.

III. MQXFA1 MAGNET ASSEMBLY

A. Real Coil Parameters

The four coils used for the real magnet were wound and cured at FNAL, then reacted and impregnated at BNL or

TABLE III
MQXFA1 COILS PARAMETERS

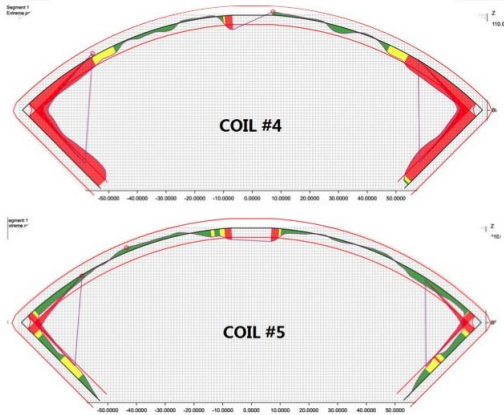| Coil ID	Geometry	Conductor	Cable ID	R & I
02	1st Gen.	0.85 mm 132/169	P35OL1060	BNL
03	2nd Gen.	0.85 mm 144/169	P47OL1064	FNAL
04	2nd Gen.	0.85 mm 132/169	P45OL1069	BNL
05	2nd Gen.	0.85 mm 108/127	P43OL1070	FNAL

Fig 9. CMM Coil profile of Coils 04 & 05 at 1940 mm from LE. Black line represents nominal geometry; red lines signify 50 μm offset either side. These profiles show Coil 04 as smaller than Coil 05.

FNAL. The coil design changed during the fabrication of these first few coils [16], and therefore these coils are not uniform in conductor or geometry. This being the case, magnetic field quality is not an aim for this first structure; rather magnet training performance is the primary goal for this magnet. See Table III for coil parameters.

Coil CMM profile measurements were taken for each coil. Visible in Fig. 9 there appears to be systematic difference in the coils that were reacted & impregnated at BNL and FNAL. This will be analyzed as more coils are produced, with potential implications to coil selection during HL-LHC AUP production. Regardless, all four coils measured smaller than nominal size.

Additionally, Coil 03 also displayed an electrical weakness to pole island segments after reaction and impregnation. These pole segments are at the opposite ends of the coil, and are not electrically connected. Therefore, it was decided to test this coil placing it as close as possible to ground in the electrical
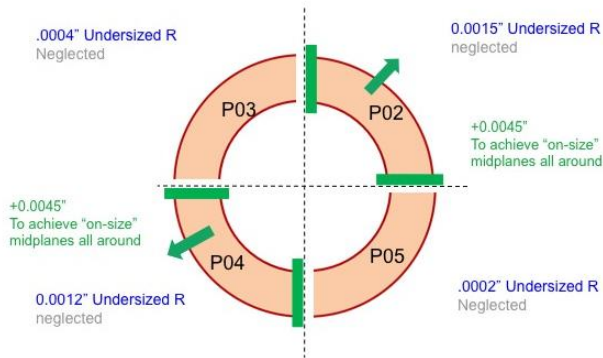

Fig. 10. Coil arrangement, viewed from the LE. Magnet electrical order is (+) 02 – 03 – 05 – 04 (-). Green represents polyimide + B-stage layers applied to midplanes.

order of the magnet; this condition would be satisfied with the coil in the 2nd or 3rd position since the magnet will be symmetrically grounded. See Fig 10 for the coil arrangement.
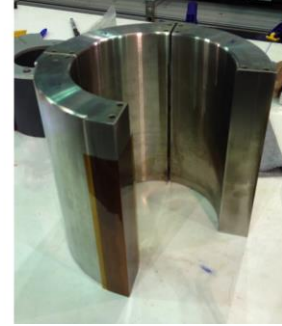

Fig 11. Segmented stainless steel extension used at the RE for the MQXFA1 magnet.

As mentioned earlier, the MQXFA1 coils are shorter than those that will be produced later. To manage this a 213 mm long stainless steel "plug" extension was placed at the RE of the coil pack while the LE of the coils remained in their nominal positions in the structure. This extension was originally made as a single cylindrical part, but electrical protection and variations in coil length necessitated sectioning it into four quadrants that could be electrically isolated from one another and the coils, and loaded independently by the axial bullets. See Figure 11.

B. Coil Pack Subassemblies

The coil pack assembly was built up a total of four times, the first two using pressure sensitive film. From the lessons learned from MQXFA1M, all the pads laminations were bolted for these two builds, which helped to develop a clearer pressure response. The final assembled coil pack, however, still bolted every 7th lamination as originally planned. The final shim package is tabulated in Table IV.

TABLE IV
FINAL RADIAL BUILD UP FOR MQXFA1 COILS

Radial Element	Coil 02	Coil 03	Coil 04	Coil 05
Coil GPI	115 μm (Polyimide + B-stage)			
Coil Specific shims*	115 μm	0	115 μm	0
Pressure Sensitive film	0			
Radial shim	2x 125 μm Polyimide + 125 μm G11			

* Applied to coil midplanes only.

1) Pole Gap Key Shimming Change

Initial results of the MQXFS magnets were suggesting a higher coil preload would be necessary to prevent detachment of the pole turn in the coils. To help achieve this the use of small gap between the pole key and collars was explored in the MQXFS5 [8], and for the MQXFA1 it was determined that leaving a small gap of 25-50 μm per side between collars and pole keys would allow the coils to achieve proper preload levels without increasing the stress in the shells, which was approaching engineering limits of the 7075 alloy [17]. Feeler
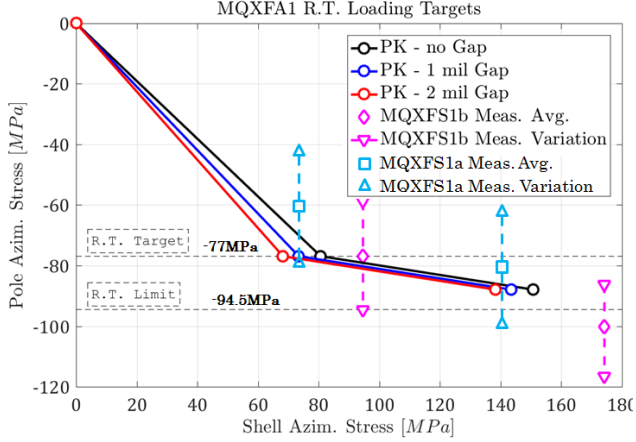
Fig. 12. Load cases for three gap conditions (0, 25 μm, 50 μm) in MQXFA1, compared with the MQXFS1a and MQXFA1b magnets, both of which did not have gaps between the keys.

gauges measurements confirmed that there was an average gap of 50 μm between the pole keys and collars of the final coil pack.

C. Magnet Integration

1) Azimuthal Preload

Figure 12 and Table V show a comparison of the loads in the various magnets. The pole key gap cases shown in Fig 12 were based on the preload explorations described above. According to the FEA simulations our target for MQXFA1 was
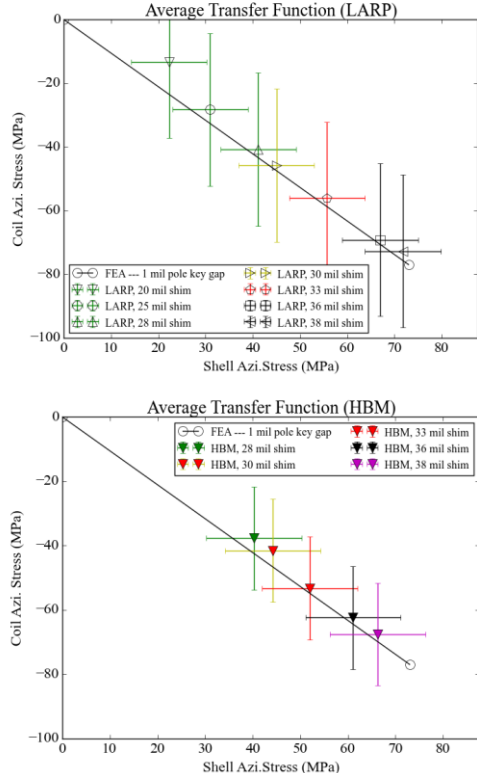

Fig. 13. Average transfer function plots of the MQXFA1 structure during loading (580 μm interference is equivalent to 38 mil). Top plot is Vishay data only; Bottom plot is HBM data only.

TABLE V
COMPARISONS OF AZIMUTHAL PRELOAD TARGETS

Cond.	Loc.	MQXFS1a	MQXFS3	MQXFS1b	MQXFA1
R.T.	Coil	-61	-73	-77	-77
	Shell	72	102	95	73
1.9 K	Coil	-81	-92	-101	-88
	Shell	140	178	173	143
				Interference	640 μm

to insert 640 μm of interference in order to achieve a strain of 1020 με in the shell at RT. This value was based on the MQXFS1b results whose loading conditions were used as a guideline: the maximum value of the measurement variations in MQXFS1b coil stresses (-94.5 MPa) was used as the limit the maximum for the MQXFA1 preload operations.

The actual amount of interference inserted was 580 μm, which corresponded to an average of 900 με in the shell and -560 με in the coils. The closure of the initial gap was seen in the knee of the plot as expected. As seen in Figure 13, the loading of the mechanical model still matched the FEA transfer function very closely. The two strain gauge systems differed with the HBM gauges reading lower values again, though likely again due to incorrect system settings applied.

2) Axial Preload

The axial preload target was designed to apply 0.61 MN (~49% of the Lorentz force) on the coil ends at 1.9 K, based again on the preliminary results seen from the MQXFS magnets. The MQXFA1 axial rods, being made of 316L stainless steel, require a higher R.T. preload than the aluminum versions due to a lower CTE. At room temperature this equates to a target of 580 με in the rods. The axial loading operation actually achieved an average of 619 με.

IV. EVALUATION OF TOOLING PERFORMANCE

A. Assembly Infrastructure

Overall, the magnet assembly tooling that was scaled up from the MQXFS experience performed as planned. In spite of the tight schedule the assembly of these two structures followed, they were completed and delivered on time. Some issues were noted, however, to be managed in future assemblies. See Table VI for a summary.

External schedule pressures also did not allow for time to have the magnetic measurements and fiducialization operations to be performed on MQXFA1 as originally planned. It is expected that after testing, when the schedule will be less impacted, magnet will be surveyed and fiducialized; this will be a crucial step in the preparations for magnet production for the project.

V. NEXT STEPS

The MQXFA1 magnet will be tested at BNL in summer 2017. The lessons learned from the assembly process are al-

TABLE VI
MQXFA Assembly Issues Status

Description	Issue	Corrected?
Infrastructure		
Shell-yoke assembly stand	Height clearances	Prior to MQXFA2
Coil pack assembly tables	Level wheel casters	Prior to MQXFA2
Coil GPI Stretcher	Stretch from both ends	Prior to MQXFA2
Yoke tension rig	Add pressure relief stop	Prior to MQXFA2
Mag. Meas./Fiducialization	Fiducialization targets designed	After MQXFA1 test
Processes		
Lamination thickness	Thickness tolerance build up	MQXFA2
Fuji paper exposure	All bolts to be used	Yes
Strain system readings	System parameters applied	Prior to MQXFA2
Magnet fiducialization	Develop process	After MQXFA1 test

ready being applied, and modifications to the assembly tooling are currently underway. Most of the issues discovered in the assembly of the MQXFA1 structures will be solved before the next structure is assembled.

Parts for this second structure, MQXFA2, are already in procurement, due to arrive in the fall of 2017. This magnet is expected to be assembled and then tested in spring 2018. This second structure will be the first prototype for the HL-LHC AUP project, and will be a strong candidate to be a "tunnel-ready" spare for the inner triplet magnets. The third structure will be the final pre-series magnet and is expected to be assembled in fall-2018.

The tooling and the processes that have been developed for this first MQXFA1 will be used to assemble the rest of the prototypes and the 20 magnet structures required for the HL-LHC AUP project.

VI. Conclusion

In this paper we reported on the assembly and mechanical performance of the MQXFA1M and MQXFA1, the first MQXFA magnet prototype for the HL-LHC AUP. The magnet was assembled and delivered on time, and the FEA simulations showed good correlation with the measured values. The test of this magnet started in late August 2017. Minor changes based on these first assemblies will refine the tooling to streamline the process for producing the 20 structures required for the HL-LHC AUP project.

References

[1] E. Todesco, H. Allain, G. Ambrosio, G. Arduini, F. Cerutti, R. De Maria, L. Esposito, S. Fartoukh, P. Ferracin, H. Felice, R. Gupta, R. Kersevan, N. Mokhov, T. Nakamoto, I. Rakno, J. M. Rifflet, L. Rossi, G. L. Sabbi, M. Segreti, F. Toral, Q. Xu, P. Wanderer, R. van Weelderen, "A First Baseline for the Magnets in the High Luminosity LHC Insertion Regions," *IEEE Trans. Appl. Supercond.* 24 (2014).

[2] P. Ferracin, *et al.*, "Development of MQXF: The Nb3Sn Low-ß Quadrupole for the HiLumi LHC," *IEEE Trans. Appl. Supercond.*, vol. 26, no. 4, June 2016.

[3] H. Felice *et al.*, "Test results of TQS03: a LARP shell-based Nb3Sn quadrupole using 108/127 conductor," *Journal of Physics: Conference Series* 234 (2010) 032010.

[4] J. F. Muratore et al., "Test results of LARP 3.6 m Nb3Sn racetrack coils supported by full-length and segmented shell structures," *IEEE Trans. Appl. Supercond.*, vol. 19, no. 3, pp. 1212–1216, Jun. 2009.

[5] G. Ambrosio et al., "Test Results and Analysis of LQS03 Third Long Nb3Sn Quadrupole by LARP", *IEEE Trans. Appl. Supercond.*, Vol. 23, No 3, June 2013.

[6] J. DiMarco, et al., "Test Results of the LARP Nb3Sn Quadrupole HQ03a," ", *IEEE Trans. Appl. Supercond.*, Vol. 26, No 4, June 2016.

[7] S. Stoynev, et al., "Summary of test results of MQXFS1 - the first short model 150 mm aperture Nb3Sn quadrupole for the High-Luminosity LHC upgrade," *presented at this conference.*

[8] G. Vallone, et al., "Mechanical Analysis of the Short Model Magnets for the Nb3Sn Low-ß Quadrupole MQXF," *presented at this conference.*

[9] S. Caspi et al., "The Use of Pressurized Bladders for Stress Control of Superconducting Magnets," *IEEE Trans. On Appl. Supercond.*, Vol. 11, No. 1 , March 2001

[10] Eddie Frank Holik, Giorgio Ambrosio, Michael Anerella, Rodger Bossert, Eugenio Cavanna, Daniel Cheng, Daniel R. Dietderich, Paolo Ferracin, Arup K. Ghosh, Susana Izquierdo Bermudez, Steven Krave, Alfred Nobrega, Juan Carlos Perez, Ian Pong, GianLuca Sabbi, Carlo Santini, Jesse Schmalzle, Peter Wanderer, Xiaorong Wang, and Miao Yu, "Fabrication of First 4-m Coils for the LARP MQXFA Quadrupole and Assembly in Mirror Structure," *IEEE Trans. Appl. Supercond.*, vol. 27, no. 4, June 2017.

[11] J. Muratore, et al., "Design and Fabrication of the 1.9 K Magnet Test Facility at BNL, and Test of the First 4m Long MQXF Coil," *presented at this conference.*

[12] H. Pan, et al., "Assembly Tests of the First Nb3Sn Low-Beta Quadrupole Short Model for the Hi-Lumi LHC," *IEEE Trans. Appl. Supercond.*, vol. 26, no. 4, June 2016.

[13] H. Pan, H. Pan, E. Anderssen, G. Ambrosio, D. W. Cheng, M. Juchno, P. Ferracin, H. Felice, J. C. Perez, S. O. Prestemon, G. Vallone, "Mechanical Design Studies of the MQXF Long Model Quadrupole for the HiLumi LHC," *IEEE Trans. Appl. Supercond.*, vol. 27, no. 4, June 2017.

[14] P. Han, "MQXFA1 preload calculation," *LBNL Eng. Note* SU-1009-1085.

[15] H. Felice, "Design of the MQXFA 1st prototype support structure." [Online]. Available: https://indico.fnal.gov/conferenceDisplay.py?confId=10094. Accessed on July 24, 2017.

[16] S. Izquierda Bermudez, et al., "Second Generation Coil Design of the Nb3Sn low-ß Quadrupole for the High Luminosity LHC, " *IEEE Trans. Appl. Supercond.*, vol. 26, no. 4, June 2016.

[17] E. C. Anderssen, "Fracture calculations MQXF Shells and Tie Rods," *LBNL Eng. Note* SU-1005-6694